

## Optical control of collisional population flow between molecular electronic states of different spin multiplicity

E. H. Ahmed,<sup>1,\*</sup> X. Pan,<sup>1</sup> J. Huennekens,<sup>2</sup> and A. M. Lyyra<sup>1</sup>

<sup>1</sup>*Department of Physics, Temple University, Philadelphia, Pennsylvania 19122, USA*

<sup>2</sup>*Department of Physics, Lehigh University, Bethlehem, Pennsylvania 18015, USA*

(Received 1 March 2014; published 16 June 2014)

In this work we demonstrate optical control of the singlet-triplet probability distribution in the outcome of a collisional process involving lithium dimers and argon atoms. The control is achieved using the Autler-Townes effect to manipulate the spin character of a spin-orbit coupled pair of levels serving as a “gateway” between the singlet and triplet electronic state manifolds.

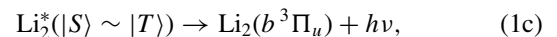
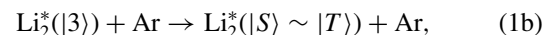
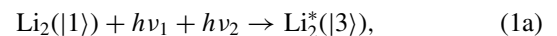
DOI: [10.1103/PhysRevA.89.061401](https://doi.org/10.1103/PhysRevA.89.061401)

PACS number(s): 34.50.Rk, 33.40.+f, 31.15.aj

The adiabatic description of molecular electronic states is based on potential energy surfaces, defined by the motion of the electrons, on which the slower nuclear motions (vibrations and rotations) occur. However, this model breaks down when relativistic effects such as the coupling between the electron spin and its orbital angular momentum (spin-orbit coupling) are taken into account. The result is that conical intersections develop between the adiabatic potential surfaces resulting in molecular states with mixed spin (multiplicity) character. A growing number of theoretical results [1–3] indicates the importance of such intersections in shaping the pathways for nonadiabatic dynamical processes. For example, conical intersections play a crucial role in the processes of intersystem crossings (nonradiative quenching) [4,5] of excited electronic states. When diatomic molecules are considered, the electronic potential energy surfaces reduce to two-dimensional curves and the conical intersections become avoided crossings of the intersecting diabatic potentials. The dipole selection rule on spin,  $\Delta S = 0$ , prohibits direct excitation between states of different spin (singlet  $\leftrightarrow$  triplet). However, nearly degenerate singlet and triplet levels, with the same rotational quantum number  $J$ , can couple together by the spin-orbit interaction, creating levels of mixed singlet-triplet character. In diatomic alkali-metal molecules, for example, such states are used in the transfer of ultracold molecules formed in the triplet  $a^3\Sigma^+$  state to deeply bound levels of the singlet ground state  $X^1\Sigma^+$  [6–8], as well as to access spectroscopically the dark triplet excited states starting from the singlet ground state  $X^1\Sigma^+$  [9–14]. Thus the use of these mixed spin-multiplicity character levels called “window” levels as intermediates in double resonance excitations allows the selection rule on spin for electric dipole transitions to be circumvented. A related, but separate phenomenon is the so-called “gateway” effect [14–17], in which transfer of population between singlet and triplet manifolds occurs by way of collisional pathways through levels of mixed character. Direct transfer of population from a pure singlet level of an alkali diatomic molecule to a pure triplet level lying very close in energy, via collisions with noble gas atoms, is an extremely weak process. Instead, it has been observed that the transfer is very much more likely

to occur in a two-step process through a mixed singlet-triplet level, even when that mixed level lies much further away in energy and has a different rotational quantum number  $J$  [14,17]. Moreover, the collisional transfer rate through the mixed levels depends critically on the degree of spin character mixing.

Recently we have demonstrated [18] that the singlet and triplet character of mutually perturbing pairs of levels coupled by the spin-orbit interaction can be optically controlled using the Autler-Townes (ac Stark) effect [19]. Building on these results, in the present work we demonstrate the optical control of *collisional* transfer between singlet and triplet states (gateway effect) of the  $\text{Li}_2$  dimer. Specifically, we consider collisions of excited  $\text{Li}_2$  molecules with argon atoms. The sequence of events in the experiment can be described by the following three reaction equations:



schematically illustrated in Fig. 1. Initially,  $\text{Li}_2$  molecules in a particular rovibrational level of the singlet ground state (level |1>) are excited by two photons (1a) through the intermediate state (level |2>) to populate the pure singlet excited state  $\text{Li}_2^*$  (|3>). In this experiment, we have used either  $G^1\Pi_g$  ( $v = 12$ ,  $J = 19$ ,  $f$ ) or  $G^1\Pi_g$  ( $v = 12$ ,  $J = 23$ ,  $f$ ) as level |3). In the second step (1b) the  $\text{Li}_2^*$  (|3>) molecules experience collisions with argon buffer gas atoms causing transfer of population to the gateway levels  $G^1\Pi_g$  ( $v = 12$ ,  $J = 21$ ,  $f$ )  $\sim 1^3\Sigma_g^-$  ( $v = 1$ ,  $N = 21$ ,  $f$ ) (|S)  $\sim$  |T). In the last step (1c), some fraction of the molecules in the gateway levels  $\text{Li}_2^*$  (|S)  $\sim$  |T) decay via spontaneous emission to the lower pure triplet state  $\text{Li}_2$  ( $b^3\Pi_u$ ). Through this collisional mechanism, the natural spin-orbit mixing in the |S)  $\sim$  |T) gateway levels allows molecules in the excited pure singlet level |3) to decay to pure triplet levels of the lower  $b^3\Pi_u$  electronic state.

We achieve optical control of the collisional transfer between the pure singlet level |3) and the pure triplet  $b^3\Pi_u$  state manifold by manipulating the spin character of the intermediate gateway levels |S)  $\sim$  |T). The change in the spin character of the components of the gateway is accomplished using the Autler-Townes (AT) effect of the coupling laser  $L_3$  (see Fig. 1). It is well known that the spin-orbit mixing of a pair of levels depends on their energy separation. We

\*Author to whom correspondence should be addressed: eahmed@temple.edu

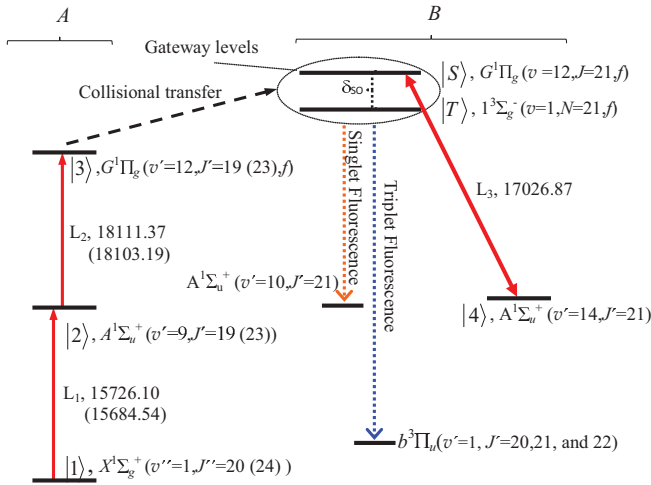


FIG. 1. (Color online) The excitation scheme for the experiment can be separated to two parts, A and B, which are connected by the collisional molecular population transfer. In part A, molecules from a thermally populated rovibrational level of the ground  $X^1\Sigma_g^+$  singlet electronic state (level  $|1\rangle$ ) are excited by laser  $L_1$  to an intermediate level  $|2\rangle$ , a rovibrational level of the  $A^1\Sigma_u^+$  singlet electronic state. Laser  $L_2$  then further excites them to level  $|3\rangle$ , a rovibrational level of the  $G^1\Pi_g$  singlet electronic state. Part B consists of the levels  $|S\rangle$ ,  $|T\rangle$ , and  $|4\rangle$ . Rotational levels of the  $G^1\Pi_g$  state (level  $|3\rangle$ ), both below [ $G^1\Pi_g(v=12, J=19, f)$ ] and above [ $G^1\Pi_g(v=12, J=23, f)$ ] the energy of the gateway levels were populated by employing two different excitation schemes for part A. As a result of collisional propensity rules ( $s \leftrightarrow a$  [14,15]), collisional transfer to the gateway levels  $|S\rangle \sim |T\rangle$  from rotational levels of the  $G^1\Pi_g$  state can be observed from levels with  $\Delta J = \pm 2, 4, \dots$  and  $f$  parity only. The resonance frequencies in the figure are given as  $\tilde{\nu} = \nu/c$  in units of  $\text{cm}^{-1}$ .

use the AT effect to shift one of the interacting levels closer (stronger coupling) or further away (weaker coupling) from the gateway partner level by controlling the power and detuning of the coupling field.

In the experiment we used a setup that is similar to the one described previously [18,20]. The  $\text{Li}_2$  dimers were produced in a five-arm heat-pipe oven loaded with lithium metal and heated to 850 K. In most quantum optics experiments collisions are unwanted and efforts are made to minimize them due to the decoherence they introduce. However, here we chose to look at the collisions explicitly. Thus, in contrast to previous experiments [18,20] in which argon gas was used in minimal amounts (100–200 mTorr) only to prevent hot metal vapor from reaching the heat-pipe oven windows, in the present work we loaded the oven with argon gas at 2 Torr pressure (measured at room temperature). Three Coherent Autoscan 699-29 dye lasers were used in the experiment. To minimize the residual Doppler linewidth, the lasers driving the first two excitations,  $L_1$  and  $L_2$ , were counterpropagating, while the control laser  $L_3$  copropagated with  $L_1$ . The beam waist  $w$  (defined as the radius at  $1/e^2$  intensity) for each laser ( $w_1 = 90 \mu\text{m}$ ,  $w_2 = 110 \mu\text{m}$ ,  $w_3 = 225 \mu\text{m}$ ) in the interaction region was measured using the razor blade technique [21]. To monitor the branching of the population between the final singlet and triplet states, we detected molecular fluorescence corresponding to

specific rovibronic transitions, collected from a  $\sim 2.5\text{-cm}$ -long interaction region, and emitted in a direction perpendicular to the laser propagation axis. The desired fluorescence was separated from the background using bandpass filtering. A SPEX 1404 double grating monochromator with bandwidth of  $\sim 0.1 \text{ nm}$  was used for the singlet channel and an interference bandpass filter (Thorlabs, center wavelength 441.6 nm and bandwidth 10 nm) was used for the triplet channel. In both cases Hamamatsu R928 photomultiplier tubes were used for detection. The powers of the pump and probe lasers were attenuated to 10 and 50 mW, respectively, using neutral density filters.

We model the experimental results using the density matrix formalism [22,23]. The equation of motion of the system is

$$\frac{d\rho}{dt} = -\frac{i}{\hbar}[H, \rho] + \Gamma\rho, \quad (2)$$

where  $\rho$  is the density matrix, and  $\Gamma$  is the relaxation matrix. In constructing the Hamiltonian matrix  $H$  we follow the description given in Ref. [18]. From the entire set of  $^7\text{Li}_2$  rotational, vibrational, and electronic states we only consider the levels that are directly coupled by the optical fields and the spin-orbit interaction, labeled  $|1\rangle$ ,  $|2\rangle$ ,  $|3\rangle$ ,  $|S_0\rangle$ ,  $|T_0\rangle$ , and  $|4\rangle$  in Fig. 1. Since levels  $|3\rangle$  and  $|S_0\rangle$  are only connected by collisional population transfer, the Hamiltonian  $H$  of the system naturally separates into two components  $H = H^1 + H^2$ . Here  $H^1$  describes the subsystem formed by the states  $|1\rangle$ ,  $|2\rangle$ , and  $|3\rangle$ , and  $H^2$  describes the subsystem formed by the states  $|S_0\rangle$ ,  $|T_0\rangle$ , and  $|4\rangle$ . In this way the original  $6 \times 6$  density matrix is replaced by two  $3 \times 3$  matrices, which simplifies the calculations significantly. The two components of  $H$  in the interaction picture have the form

$$H_I^1 = -\hbar\Delta_1|2\rangle\langle 2| - \hbar(\Delta_1 + \Delta_2)|3\rangle\langle 3| + \frac{\hbar}{2}\Omega_1(|2\rangle\langle 1| + |1\rangle\langle 2|) + \frac{\hbar}{2}\Omega_2(|3\rangle\langle 2| + |2\rangle\langle 3|), \quad (3a)$$

$$H_I^2 = -\hbar\Delta_3|4\rangle\langle 4| + \frac{\hbar}{2}\Omega_3(|4\rangle\langle S_0| + |S_0\rangle\langle 4|) + \hbar\alpha\beta\delta_{\text{SO}}(|S_0\rangle\langle T_0| + |T_0\rangle\langle S_0|). \quad (3b)$$

Equations (3a) and (3b) incorporate the rotating wave approximation [23] and are written in the basis set of the unperturbed levels. Here  $\Delta_i \equiv \omega_i - \omega_{\text{res}}$  are the detunings for molecules at rest in the lab frame.  $\omega_i$  is the frequency of the  $i$ th laser and  $\omega_{\text{res}}$  is the resonance transition frequency between the corresponding unperturbed levels.  $\Omega_i$  is the Rabi frequency of the  $i$ th laser, defined as  $\Omega_i = \frac{\mu \cdot E_i}{\hbar}$ , with  $\mu$  the dipole matrix element of the corresponding transition.  $\delta_{\text{SO}}$  is the experimentally measured separation in energy between the mixed levels  $|S\rangle$  and  $|T\rangle$ . The mixed spin-orbit coupled states  $|S\rangle = \alpha|S_0\rangle - \beta|T_0\rangle$  and  $|T\rangle = \alpha|T_0\rangle + \beta|S_0\rangle$  ( $\alpha^2 + \beta^2 = 1$ ) arise as a result of the spin-orbit interaction between the closely spaced pair of levels  $|S_0\rangle$  and  $|T_0\rangle$ . The separation between the unperturbed levels  $\delta_{\text{SO}}^0$  is proportional to  $\delta_{\text{SO}}$ :  $\delta_{\text{SO}}^0 = (\alpha^2 - \beta^2)\delta_{\text{SO}}$  [18,24].

Due to the existing spin-orbit coupling present between the levels  $|S\rangle$  and  $|T\rangle$  when only the weak pump and the probe lasers are present, a fraction of the molecules excited to level  $|3\rangle$  naturally decay through the mixed levels  $|S\rangle \sim |T\rangle$  to the pure triplet state  $b^3\Pi_u$ . In Fig. 2(a) we show this triplet

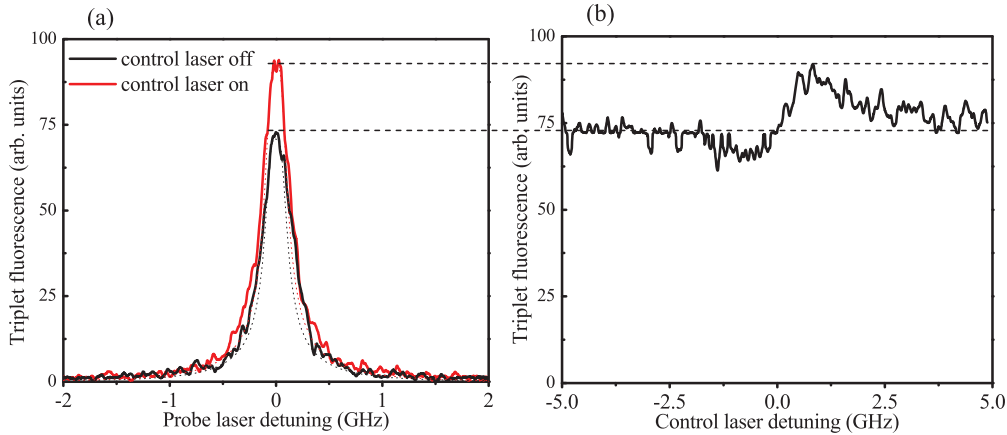


FIG. 2. (Color online) Triplet fluorescence from the gateway levels  $1^3\Sigma_g^-(v=1, N=21, f) \sim G^1\Pi_g(v=12, J=21, f)$ ; (a) Probe laser ( $L_2$ ) scan with the control laser ( $L_3$ ) fixed on resonance, (b) control laser scan while the probe laser was fixed on resonance. The excitation scheme from level |1> to level |3> (part A in Fig. 1) is  $X^1\Sigma_u^+(v''=1, J''=20) \rightarrow A^1\Sigma_u^+(v'=11, J'=19) \rightarrow G^1\Pi_g(v=12, J=19, f)$ . In (a), the experimental scans and the simulations are shown by solid and dashed lines, respectively. The signal is detected as fluorescence to the  $b^3\Pi_u(v'=1, J'=20, 21, 22)$  levels.

fluorescence (black trace) as a function of the probe laser detuning from resonance. When we introduce the control laser ( $L_3$ ), enhancement in the collisionally mediated transfer of population between the singlet level |3> and the triplet  $b^3\Pi_u$  levels can be observed [red (light gray) trace]. The increase in the transfer is a result of the enhanced mixing between the singlet and the triplet states caused by the Autler-Townes effect of the control laser. In Fig. 2(b) we illustrate the transfer rate as a function of the detuning of the control laser. The peak position corresponds to the resonance, while the decrease in transfer rate observed at lower frequency is from the nonresonant ac Stark shift experienced by the singlet component of the pair which causes the levels to separate and thus mix less. From the relative change in the intensity of the triplet fluorescence observed in Fig. 2 by the action of the control laser we estimate that the suppression (for negative detuning) and enhancement (for resonance or positive detuning) in the singlet to triplet ( $|3\rangle \rightarrow b^3\Pi_u$ ) transfer is approximately 11% and 20%, respectively. Since the total molecular population in the relevant levels is unaffected by the control laser this translates to a similar relative change in the rate constant of the overall collisional singlet to triplet transfer process.

In Fig. 3 we show the effect of the control laser power on the transfer rate. We observe that the increase in the control laser power (Rabi frequency) leads to enhancement in the transfer rate, because of the increased spin-orbit coupling of the gateway levels. Since the molecular population is conserved, while the transfer to the triplet manifold ( $b^3\Pi_u$ ) is enhanced, the decay to the singlet manifold ( $A^1\Sigma_u^+$ ) must decrease. To test this, we have performed an experiment in which we simultaneously recorded the triplet and the singlet fluorescence from the gateway levels as shown in Fig. 4. As is evident from the figure, the singlet and triplet fluorescence signals from the gateway are complementary. When the triplet transfer is enhanced ( $L_3$  near resonance or blue detuned), the singlet transfer is suppressed and vice versa ( $L_3$  red detuned from resonance). The lower signal to noise ratio in this figure in comparison to the data shown in Figs. 2 and 3 is due to

our use of a SPEX 1404 monochromator (50- $\mu\text{m}$  entrance and exit slits) in the role of a very narrow bandpass filter for the observation of the singlet fluorescence and the low laser power for the lasers  $L_1$  and  $L_2$ . The latter was necessitated by the experimental difficulty in isolating the gateway singlet fluorescence  $1^3\Sigma_g^-(v=1, N=21, f) \sim G^1\Pi_g(v=12, J=21, f) \rightarrow A^1\Sigma_u^+(v'=10, J'=21)$  from the fluorescence from the directly populated level |3> [ $G^1\Pi_g(v=12, J=23, f) \rightarrow A^1\Sigma_u^+(v'=10, J'=23)$ ] (see Fig. 5).

The simulations based on Eqs. (2) and (3) shown in Figs. 2 and 4 agree well with the experiment, confirming our interpretation of the results. Since the experiment focuses on the population redistribution due to collisions, the relaxation processes such as spontaneous decay, collisions, and laser

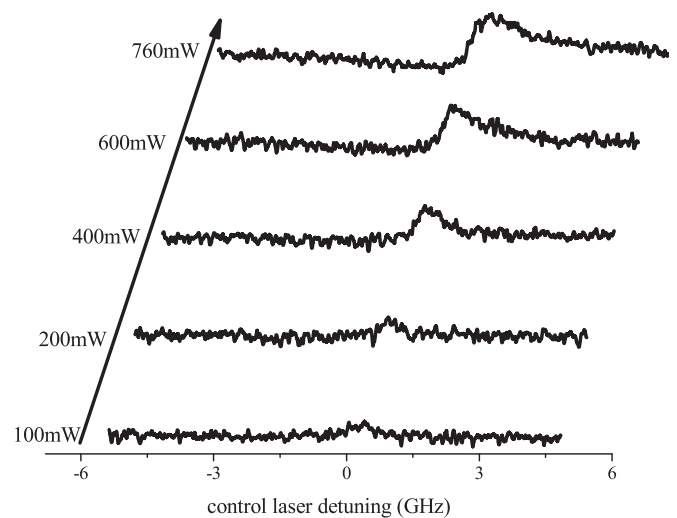


FIG. 3. Dependence of the collisional transfer rate on the power of the control laser. The control laser is scanned over the  $1^3\Sigma_g^-(v=1, N=21, f) \sim G^1\Pi_g(v=12, J=21, f) \leftrightarrow A^1\Sigma_u^+(v'=14, J'=21)$  resonance, while the pump and probe lasers are kept on resonance. The excitation scheme is the same as in Fig. 2.

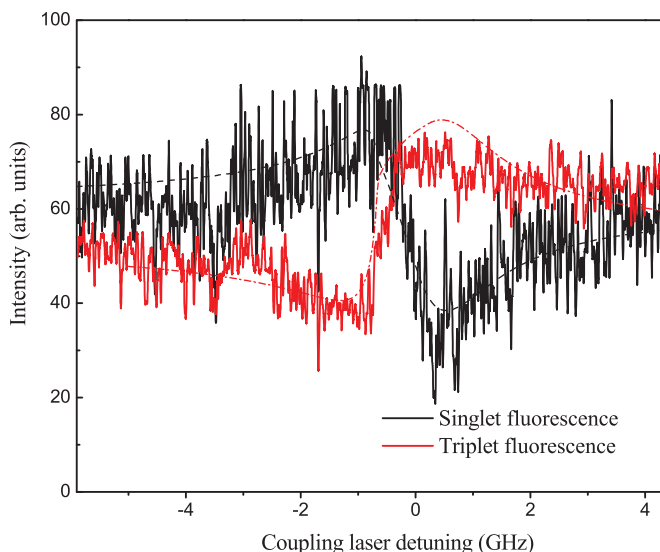


FIG. 4. (Color online) Simultaneous observation of the singlet and triplet components of the gateway as functions of the coupling laser detuning. The excitation scheme from level  $|1\rangle$  to level  $|3\rangle$  (part A in Fig. 1) is  $X^1\Sigma_g^+(v''=1, J''=24) \rightarrow A^1\Sigma_u^+(v'=11, J'=23) \rightarrow G^1\Pi_g(v=12, J=23, f)$ . The experimental scans and the simulations are shown by solid and dashed lines, respectively.

beam transit play a critical role in the model. They are incorporated into the model as phenomenological parameters via the matrix  $\Gamma$  in Eq. (2). The spontaneous decay rate,  $W_j = 1/\tau_j$ , of level  $j$ , which is inversely proportional to its lifetime, is calculated from experimental molecular potentials and transition dipole moment functions. We estimate the total collisional relaxation rate (quenching rate),  $\Gamma_Q$ , of a particular level, by calculating the average time between collisions  $t_c = l/v$  and assuming that  $\Gamma_Q = 1/t_c$ . Here  $l = \frac{kT}{\sqrt{2\pi dP}}$  is the average mean free path of the  $\text{Li}_2$  molecules and  $v = \sqrt{\frac{2kT}{m}}$  is the most probable speed. We assume that all levels involved in the experiment have the same quenching rate of  $\Gamma_Q = 7.35 \times 10^{-7} \text{ s}^{-1}$ , calculated using the following values for the parameters:  $T = 850 \text{ K}$ ,  $P = 5831 \text{ mTorr}$  (obtained from  $P_{\text{Ar}}(293 \text{ K}) = 2000 \text{ mTorr}$ , and  $P_{\text{Li}}(850 \text{ K}) = 28.9 \text{ mTorr}$  [25]), and  $d = 2.67 \text{ \AA}$  (the equilibrium internuclear distance of the ground state of  $\text{Li}_2$  [26]). This value for  $\Gamma_Q$  is in good agreement with an experimentally measured quenching rate for NaK molecules [27]. The most important collisional rate for our experiment is the collisional population transfer rate from level  $|3\rangle$  to the  $|S\rangle \sim |T\rangle$  mixed gateway, which is only a fraction of the total collisional quenching rate  $\Gamma_Q$  of level  $|3\rangle$ . We calculated the branching ratio for the process

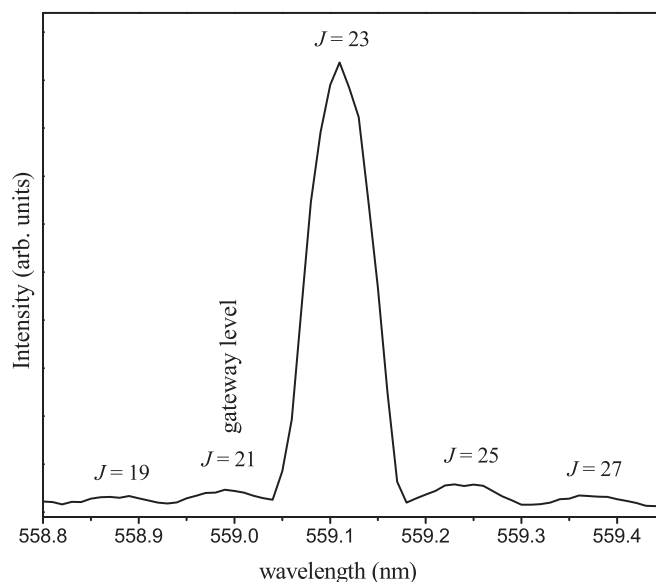


FIG. 5. Resolved fluorescence of the direct excitation  $X^1\Sigma_g^+(v''=1, J''=24) \rightarrow A^1\Sigma_u^+(v'=9, J'=23) \rightarrow G^1\Pi_g(v=12, J=23, f)$  and its  $\Delta J = \pm 2, \pm 4$  collisional satellite components. The  $\Delta J = -2$  component is the mixed pair of gateway level  $1^3\Sigma_g^-(v=1, N=21, f) \sim G^1\Pi_g(v=12, J=21, f)$ .

$|3\rangle \rightarrow |S\rangle \sim |T\rangle$  from  $\Gamma_Q$  and the experimentally measured fluorescence ratio of the collisional satellite  $G^1\Pi_g(v=12, J=21, f) \rightarrow A^1\Sigma_u^+(v'=10, J'=21)$  line intensity to the direct  $G^1\Pi_g(v=12, J=23, f) \rightarrow A^1\Sigma_u^+(v'=10, J'=23)$  line intensity (see Fig. 5) and the rate equation model given in Ref. [27].

In conclusion, we have demonstrated optical control of the collisional population flow between singlet and triplet state manifolds. The control is achieved by manipulating the spin character in a pair of singlet-triplet mixed gateway levels using the Autler-Townes effect. Thus we show that the rate coefficient of a collisional process between excited molecules ( $^7\text{Li}_2$ ) and atoms (Ar) leading to internal state changes in the molecules, can be effectively manipulated with a laser. More significant enhancements of collisional population transfer through the gateway can be achieved by using larger Rabi frequencies with a pulsed laser. In addition, gateway levels can be created from singlet and triplet levels that hardly interact to begin with.

We gratefully acknowledge financial support from NSF Grants No. PHY 0855502, No. PHY 1205903, and No. PHY 0968898, and the Lagerqvist Fund of Temple University.

- [1] S. Mahapatra, *Acc. Chem. Res.* **42**, 1004 (2009).
- [2] G. W. Richings and G. A. Worth, *J. Phys. Chem. A* **116**, 11228 (2012).
- [3] D. Townsend, B. J. Sussman, and A. Stolow, *J. Phys. Chem. A* **115**, 357 (2011).
- [4] W. M. Gelbart and K. F. Freed, *Chem. Phys. Lett.* **18**, 470 (1973).

- [5] G. W. Robinson, *J. Chem. Phys.* **47**, 1967 (1967).
- [6] J. M. Sage, S. Sainis, T. Bergeman, and D. DeMille, *Phys. Rev. Lett.* **94**, 203001 (2005).
- [7] K. K. Ni, S. Ospelkaus, M. H. G. de Miranda, A. Pe'er, B. Neyenhuis, J. J. Zirbel, S. Kotochigova, P. S. Julienne, D. S. Jin, and J. Ye, *Science* **322**, 231 (2008).

- [8] J. G. Danzl, E. Haller, M. Gustavsson, M. J. Mark, R. Hart, N. Bouloufa, O. Dulieu, H. Ritsch, and H. C. Nagerl, *Science* **321**, 1062 (2008).
- [9] L. Li and R. W. Field, *J. Phys. Chem.* **87**, 3020 (1983).
- [10] L. Li and R. W. Field, in *Molecular Dynamics and Spectroscopy of Stimulated Emission Pumping*, edited by H. L. Dai and R. W. Field (World Scientific, Singapore, 1995), Chap. 7, p. 251.
- [11] L. Li and A. M. Lyyra, *Spectrochim. Acta, Part A* **55**, 2147 (1999).
- [12] L. Morgus, P. Burns, R. D. Miles, A. D. Wilkins, U. Ogba, A. P. Hickman, and J. Huennekens, *J. Chem. Phys.* **122**, 144313 (2005).
- [13] P. Burns, L. Sibbach-Morgus, A. D. Wilkins, F. Halpern, L. Clarke, R. D. Miles, L. Li, A. P. Hickman, and J. Huennekens, *J. Chem. Phys.* **119**, 4743 (2003).
- [14] H. Lefebvre-Brion and R. W. Field, *The Spectra and Dynamics of Diatomic Molecules* (Elsevier, Amsterdam, 2004).
- [15] M. H. Alexander, *J. Chem. Phys.* **76**, 429 (1982).
- [16] L. Li, Q. S. Zhu, A. M. Lyyra, T. J. Whang, W. C. Stwalley, R. W. Field, and M. H. Alexander, *J. Chem. Phys.* **97**, 8835 (1992).
- [17] L. Li, S. Antonova, A. Yiannopoulou, K. Urbanski, and A. M. Lyyra, *J. Chem. Phys.* **105**, 9859 (1996).
- [18] E. H. Ahmed, S. Ingram, T. Kirova, O. Salihoglu, J. Huennekens, J. Qi, Y. Guan, and A. M. Lyyra, *Phys. Rev. Lett.* **107**, 163601 (2011).
- [19] S. H. Autler and C. H. Townes, *Phys. Rev.* **100**, 703 (1955).
- [20] E. Ahmed, A. Hansson, P. Qi, T. Kirova, A. Lazoudis, S. Kotochigova, A. M. Lyyra, L. Li, J. Qi, and S. Magnier, *J. Chem. Phys.* **124**, 084308 (2006).
- [21] D. R. Skinner and R. E. Whitcher, *J. Phys. E* **5**, 237 (1972).
- [22] S. Stenholm, *Foundations of Laser Spectroscopy* (Wiley Interscience, New York, 1984).
- [23] M. O. Scully and M. S. Zubairy, *Quantum Optics* (Cambridge University Press, Cambridge, 2002).
- [24] T. Kirova and F. C. Spano, *Phys. Rev. A* **71**, 063816 (2005).
- [25] A. N. Nesmeyanov, *Vapor Pressure of the Chemical Elements* (Elsevier, Amsterdam, 1963).
- [26] X. J. Wang, J. Magnes, A. M. Lyyra, A. J. Ross, F. Martin, P. M. Dove, and R. J. Le Roy, *J. Chem. Phys.* **117**, 9339 (2002).
- [27] C. M. Wolfe, S. Ashman, J. Bai, B. Beser, E. H. Ahmed, A. M. Lyyra, and J. Huennekens, *J. Chem. Phys.* **134**, 174301 (2011).